JMEPEG
https://doi.org/10.1007/s11665-023-08395-2

1059-9495/$19.00

TECHNICAL ARTICLE

An Investigation of 3D Printing Parameters on Tensile Strength of PLA Using Response Surface Method

Mehmet Masum Tünçay

Submitted: 17 April 2023 / Revised: 20 May 2023 / Accepted: 30 May 2023

Additive manufacturing has many techniques and has been frequently used and studied recently. The fused deposition modeling (FDM) method, which is one of these techniques, is a widely used three-dimensional (3D) printing method that works with the extrusion principle. The parameters used during printing affect the properties of the final product. This study investigated the effect of print angle, infill density, and perimeter count parameters on the tensile strength characteristics of FDM-printed PLA samples by the response surface method (RSM), an experimental design method. The tensile strengths of the samples produced according to the test lists obtained using the Box–Behnken design were determined. A model equation showing the effect of the relevant parameters was created. From the experiments, the compatibility of the model equation with the experimental results has been demonstrated. The highest tensile strength values were achieved in cases where the print angle was 90°, the infill density was 100%, and the number of walls was 5-6.

Keywords 3-D printing, FDM, PLA, RSM, tensile strength

1. Introduction

Additive manufacturing (AM) is a production method that has become very popular recently. It is a technology for printing the part obtained digitally with the help of CAD programs into the required file format (.stl) and then printing it with the relevant production device (Ref 1, 2). It is based on digitally cutting three-dimensional (3D) models obtained on the computer into cross sections and then adding them layer by layer to obtain the final part (Ref 3). There are different AM techniques, such as stereolithography (SLA), fused deposition modeling (FDM), laminated object manufacturing (LOM), direct light processing (DLP), polyjet (PJ), selective laser sintering (SLS), selective laser melting (SLM), electron beam melting (EBM), and binder jetting (BJ) (Ref 2, 4, 5). FDM is one of the most common methods and is predominantly a technology for melting and extruding polymer filaments (Ref 6, 7). Polylactic acid (PLA), acrylonitrile butadiene styrene (ABS), polycarbonate (PC), polyethylene terephthalate glycol-modified (PETg), and polypropylene (PP) are the most preferred materials to be printed with FDM (Ref 8-10). Additionally, recycled polymeric materials such as low-density polyethylene (LDPE) are potential candidates to be used as filaments for FDM processes (Ref 11). Some important properties of PLA are biocompatibility, biodegradability, good surface roughness, and low cost (Ref 12, 13). The parameter selections to be made during the printing of parts with the FDM process affect the final properties such as mechanical, the printing time, and the amount of material used (Ref 14-16). For example, Mohamed et al. (Ref 17) stated that layer thickness, air gap, and the number of contours were the most influential parameters on the dynamic mechanical properties of samples printed with FDM using PC/ABS mixed filament. Wang et al. (Ref 18) investigated the effects of parameters such as printing angle, layer thickness, infill ratio, and nozzle temperature on the tensile and dynamic mechanical properties of PLA samples printed with FDM. They concluded that the printing angles above 45° lead to breaking in layers, layer thickness affects the bonding strength between layers, a high infill ratio provides tighter bonding between layers, and high nozzle temperature causes too much liquidification in PLA. In contrast, low nozzle temperatures negatively affect fluidity and weaken layer bonding. Demircioglu et al. examined the effect of infill patterns on the tensile strength of PLA printed with FDM at a constant infill density and concluded that hexagonal infill pattern gave the highest strength (Ref 19). Gebisa et al. (Ref 20) examined the effects of the air gap, scanning width, scanning angle, number of contours and width used during FDM on the tensile properties of ULTEM 9085 polymer material and showed that the scanning angle had the most effect. Kamer et al. (Ref 21) investigated the effect of different printing speeds during the FDM process on the properties of the printed ABS and PLA samples. They concluded that the increase in printing speeds did not cause a significant change for ABS material but negatively affected the obtained properties of PLA material. Doğan and Kamer (Ref 22) stated that printing angle, nozzle diameter and layer thickness parameters had a significant effect on the creep properties of PLA test specimens printed with the FDM method. An experimental design approach is used to determine the optimum parameters that will maximize a feature affected by different process parameters, with a smaller number of experiments and a higher accuracy (Ref 23). The response surface method (RSM) is one of the experimental design methods, and the Box–Behnken design belonging to this

Mehmet Masum Tünçay, Department of Metallurgical and Materials Engineering, Faculty Engineering, Marmara University, Istanbul, Turkey. Contact e-mail: mehmet.tuncay@marmara.edu.tr.

Published online: 08 June 2023

method stands out as a more efficient approach (Ref 24, 25). The novelty of the current manuscript is based on the evaluation of the Box–Behnken experimental design approach for its usage in the estimation of the tensile strength properties of FDM-printed parts with different parameters.

Many device brands on the market print use the FDM method. Although open-source Ultimaker Cura software allows changes on many printing parameters and is only available for certain device brands, existing brands also have their own software. Zaxe (Istanbul, Turkey) is a device manufacturer that prints with the FDM method. This study aims to examine the effect of production parameters on the tensile strength (TS) of PLA material printed with Zaxe X1. The parameters that Zaxe Desktop allows to change include printing angle, layer thickness, infill density, perimeter count, top solid layer count, and bottom solid layer count. The effects of printing angle, infill density, and perimeter count on the tensile strength of PLA were investigated using the Box–Behnken design of the response surface method (RSM), an experimental design approach.

2. Experimental Method

2.1 3D Printer and Material

This study used a Zaxe X1 (Istanbul, Turkey) model desktop FDM-type printer with a 200 × 200 × 220 mm printing area. The corresponding printer is shown in Fig. 1. The PLA filament was supplied from Zaxe and had a diameter of 1.75 mm.

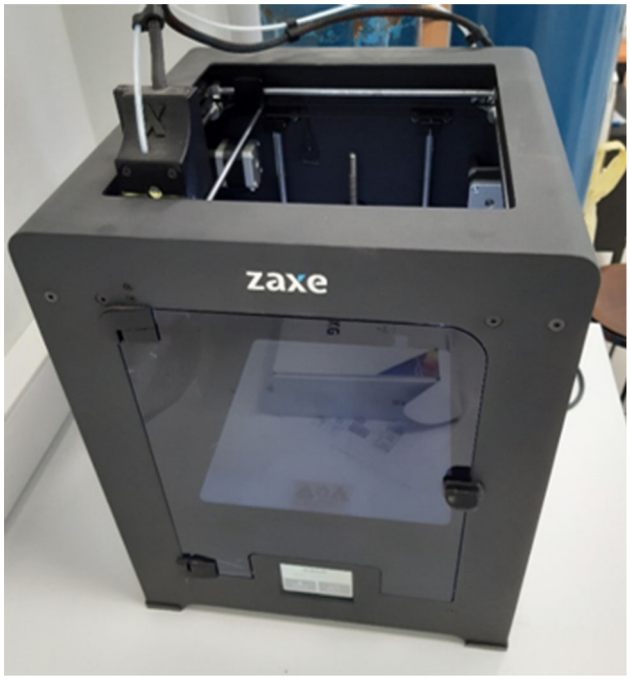

Fig. 1 The 3D printer used in this study, Zaxe X1

2.2 Experimental Design

The Box–Behnken design matrix of the RSM by the Design Expert program was used to determine the printing parameters that optimize the tensile strength (Ref 24). In this study, the three-factor Box–Behnken design was applied, and the independent variables used are given in Table 1. The device parameters other than these were used the same for each printing (layer thickness: 0.2 mm, top solid layer count: 4, bottom solid layer count: 4).

Coded values (X_i) ranging from − 1 to + 1 were used for each factor to create experimental design matrices. These coded values are obtained with the following equations by using the actual levels (x_i), the real value in the middle and the increment amount of the factor:

$$X_1 = \frac{x_1 - 45}{45} \quad \text{(Eq 1)}$$

$$X_2 = \frac{x_2 - 60}{40} \quad \text{(Eq 2)}$$

$$X_3 = \frac{x_3 - 5}{3} \quad \text{(Eq 3)}$$

where 1 refers to printing angle, 2 refers to infill density, and 3 refers to perimeter count. The perimeter count refers to the number of layers surrounding the outer surface before the inner region is filled during printing. Printing angle, infill density, and perimeter count levels are schematically shown in Fig. 2, 3 and 4, respectively.

2.3 Tensile Test

The "Type IV" sample specified in ASTM D638-14 tensile test standards for plastics was drawn in the SolidWorks program, converted into .stl format, and prepared for printing on the Zaxe X1 printer via the Zaxe Desktop program. In Fig. 5, the "Type IV" tensile test sample specified in the ASTM D638-14 standard is given schematically. Figure 6 shows the SolidWorks drawing. Tensile tests were carried out at room temperature using an electromechanical tensile test device (ALŞA Laboratory Devices Ltd. Şti., Istanbul, Turkey) with a load capacity of 1 kN and a test speed of 5 mm/min specified in ASTM D638-14 standards. The device used for the tensile tests is shown in Fig. 7.

3. Results and Discussion

The list of the experiments obtained according to the experimental design matrix and the values of the related tensile strength (TS) response are given in Table 2.

The tensile strength (TS) results corresponding to each test were entered into the Design Expert program, and the RSM analysis was carried out. The model equation was obtained over the coded values with the second-order polynomial as follows:

$$\begin{aligned} TS = {} & 53.89 + 3.93 \cdot A + 4.73 \cdot B + 6.35 \cdot C - 1.14 \cdot A \cdot B \\ & - 0.69 \cdot A \cdot C - 5.17 \cdot B \cdot C + 0.014 \cdot A^2 - 0.90 \cdot B^2 \\ & - 8.88 \cdot C^2 \end{aligned} \quad \text{(Eq 4)}$$

Table 1 The parameters of independent variables of the 3D printing experiment

		The levels (− 1,0,1) and corresponding actual values of the coded factors		
Factors	**Parameters**	**− 1**	**0**	**1**
A	Printing angle	0	45	90
B	Infill density	20	60	100
C	Perimeter count	2	5	8

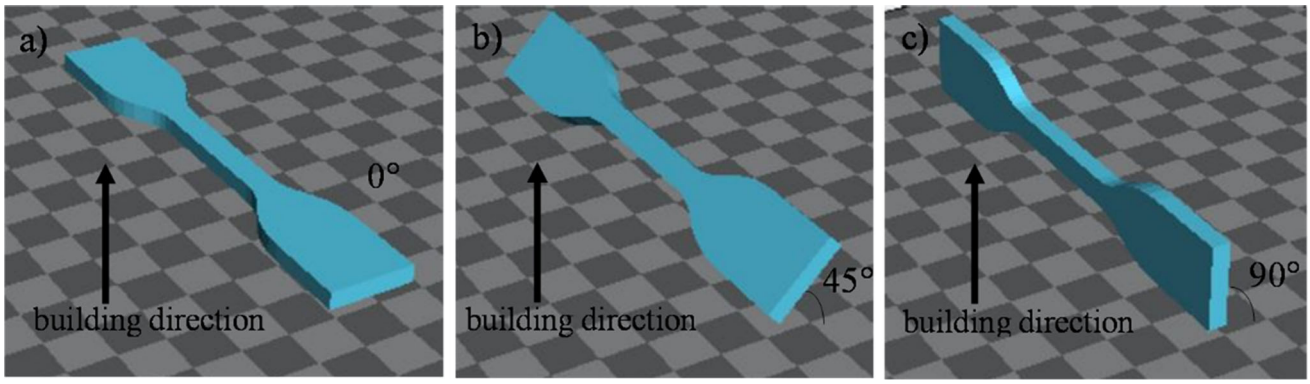

Fig. 2 Schematic view of the levels of print angle (a) 0°, (b) 45°, and (c) 90°

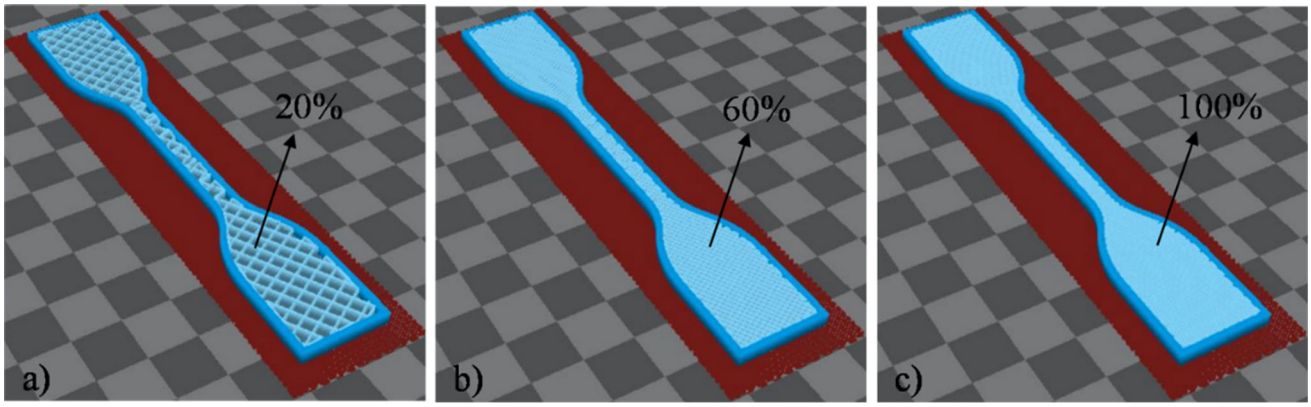

Fig. 3 Schematic view of the levels of infill density (a) 20, (b) 60, and (c) 100%

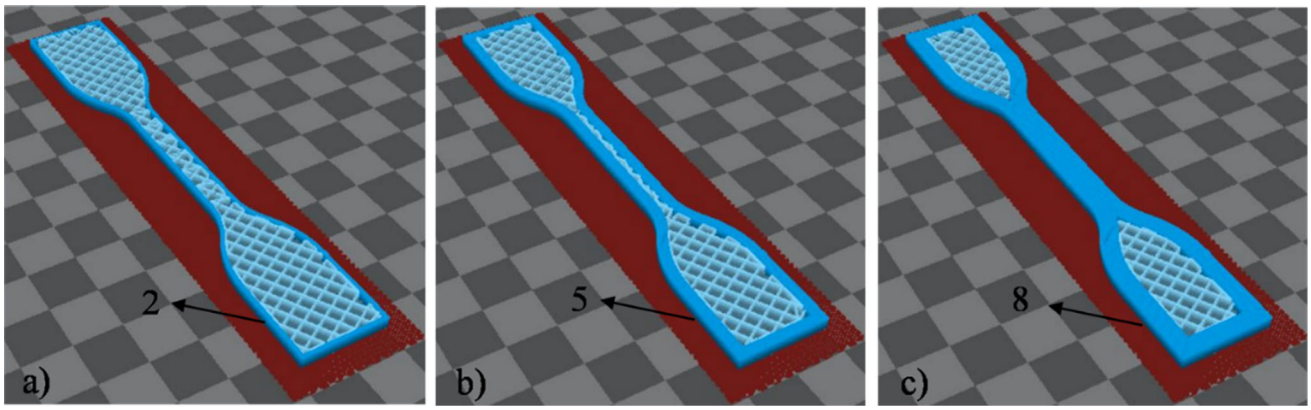

Fig. 4 Schematic view of the levels of perimeter count (a) 2, (b) 4, and (c) 8

where A, B, and C are printing angle, infill density, and perimeter count, respectively. The model was statistically evaluated with the ANOVA technique, and the results are given in Table 3. The p-value of the model was obtained as 0.0046. The model is statistically significant if this value is below 0.05 (Ref 26). When the R_2 value of the model is close to 1, it indicates that the model equation is compatible with the experimental results (Ref 27-29). Since the R2 value obtained in this study is 0.9184, it shows that the relevant model equation can be used.

The relationship between the predicted values for the tensile strength response and the actual values is given in Fig. 8, and the agreement between the results can be seen. Therefore, it can be said that the Box–Behnken method is suitable for examining the tensile strength response.

Response surface plots and contour plots were obtained to show the relationships of the independent variables with the response and are shown in Fig. 9. The third variable, not included in the axes, is fixed at the center level (0) while these graphs are produced. When the obtained plots are examined, it is seen that the tensile strength increases as the printing angle and infill density move toward the upper limits of the experimental design levels. The perimeter count also contributes positively to the strength.

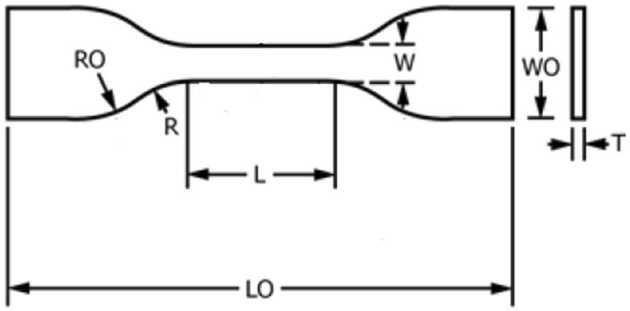

Fig. 5 Schematical view of the tensile test specimen according to the ASTM D638-14 standard (T = 4, W = 6, WO = 19, L = 33, LO = 115, R = 4, RO = 25 mm)

The tensile strength of the parts becomes higher when the printed samples are loaded perpendicular to the deposition direction of the layers (Ref 30). Considering the tensile specimens produced in this study, regardless of the printing angle, the deposition direction of the layers is perpendicular to the applied tensile force direction (Fig. 10). However, an improvement in tensile strength was observed when the

Fig. 7 The view of the tensile test device

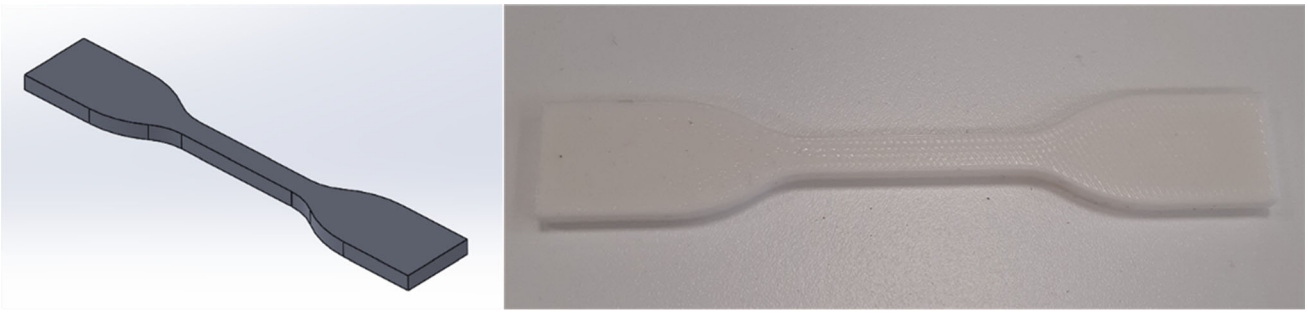

Fig. 6 The tensile test specimen that is drawn in SolidWorks and printed by 3D printer

Table 2 Experiment list for the Box–Behnken experimental design matrix and the corresponding response of tensile strength

Run	Actual level of factors			Coded level of factors			Response, TS	Printing time, min
	Printing angle	Infill density	Perimeter count	Printing angle	Infill density	Perimeter count		
1	0	20	5	− 1	− 1	0	44.58	39
2	90	20	5	1	− 1	0	56.18	53
3	0	100	5	− 1	1	0	52.12	45
4	90	100	5	1	1	0	59.15	53
5	0	60	2	− 1	0	− 1	32.12	40
6	90	60	2	1	0	− 1	39.91	49
7	0	60	8	− 1	0	1	51.50	44
8	90	60	8	1	0	1	56.55	53
9	45	20	2	0	− 1	− 1	28.42	76
10	45	100	2	0	1	− 1	52.42	87
11	45	20	8	0	− 1	1	46.14	89
12	45	100	8	0	1	1	49.46	89
13	45	60	5	0	0	0	53.89	88
14	45	60	5	0	0	0	53.89	88
15	45	60	5	0	0	0	53.89	88
16	45	60	5	0	0	0	53.89	88
17	45	60	5	0	0	0	53.89	88

Table 3 ANOVA results of the proposed model

Source	Sum of squares	df	Mean square	F-value	p-value (Prob > F)
Model	1080.36	9	120.04	8.75	0.0046
A-Printing angle	123.80	1	123.80	9.03	0.0198
B-Infill density	178.89	1	178.89	13.04	0.0086
C-Perimeter count	322.33	1	322.33	23.50	0.0019
AB	5.22	1	5.22	0.38	0.5568
AC	1.88	1	1.88	0.14	0.7224
BC	106.92	1	106.92	7.80	0.0268
A^2	7.961E−004	1	7.961E−004	5.804E−005	0.9941
B^2	3.38	1	3.38	0.25	0.6347
C^2	332.30	1	332.30	24.23	0.0017
Residual	96.01	7	13.72		
Lack of fit	96.01	3	32.00		
Pure error	0.000	4	0.000		
R^2	0.9184				

printing angle was 90°. When the raster angle, which forms the inner region, is 0° in the samples printed with FDM, it ensures that the filament is aligned along its length parallel to the loading direction of the material, resulting in stronger mechanical properties (Ref 20, 31, 32). In this study, the scanning angle is used as 45° by the device. When the printing angle is 0°, the filling part with a fixed 45° scanning angle in the inner region becomes more prominent. However, since the extruded PLA filament inside the samples with a 90° printing angle remains in a narrower area with a fixed 45° scanning angle, additive layers are formed so that it can remain more parallel to the direction in which the tensile force will be applied (Fig. 11). This may be because when the printing angle is 90°, a narrower cross-sectional area rises along the building direction; however, the same perimeter count is used, and this area is more fully composed of fibers parallel to the drawing direction. Therefore, the high strength values obtained in the samples printed with 90° in this study can be associated with this situation.

As shown from the contour plots in Fig. 9, the higher the filling density and the higher the strength. Infill density has a positive effect on strength as it reduces voids (Ref 33, 34). However, the increase in filling density causes more material consumption and prolongs printing times. Therefore, using a fill ratio that can provide the required strength using the corre-

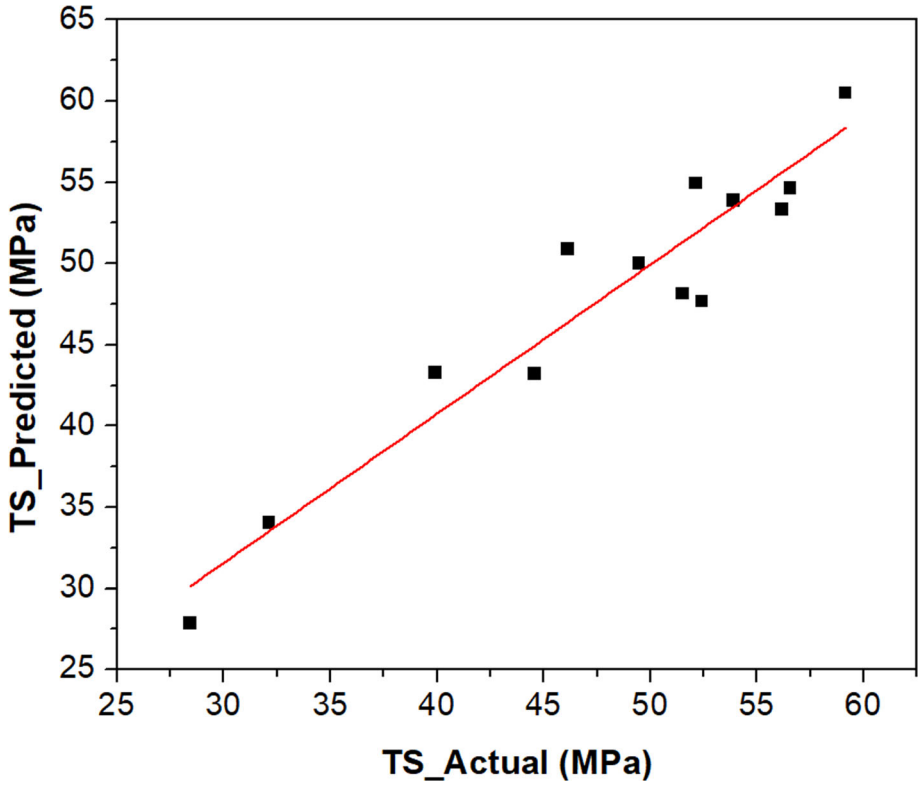

Fig. 8 The plot of predicted vs. actual values of the tensile strength

sponding response surface plots or contour plots may be appropriate.

The use of the perimeter has a positive effect on obtaining the desired geometry of the printed part, preventing gradual transitions in the curved regions and thus prevents the formation of sharp edges (Ref 35). This contributes to the positive effect of using the perimeter count on the tensile strength. Lubombo and Huneault (Ref 36) stated that increasing the number of walls from 1 to 3 increased the tensile strength of samples with the same infill pattern and density. In addition, this increase is thought to occur since the perimeters surrounding the inner layer and aligned in the tensile direction also carry the stress on the sample (Ref 36). Gebisa and Lemu (Ref 20) also stated that increasing the number of walls from 1 to 5 positively affected the strength values due to the filaments added longitudinally parallel to the loading direction. However, in some cases, the increase in the number of walls may reduce the effect of the inner zone as it causes interaction with the filled inner zone (Ref 14). In this study, it was also observed that the number of perimeters positively affected the tensile strength. Since the device automatically uses the scanning angle of 45°, the increase in the number of perimeters ensures that the fill layer with a 45° scanning angle in the inner region decreases in quantity along the section thickness and is replaced by fibers parallel to the loading axis. This effect starts to appear at lower perimeter numbers due to thinner section thickness along the loading direction in samples with 90° printing angle. When the number of perimeters exceeds 4 in the sample with a 90° printing angle, there is no space for the filling part by the scanned filaments in the inner region and only filaments that form the perimeter are in the structure parallel to the loading direction (Fig. 12). A similar situation occurs when the perimeter counts reaches 6 in the sample with 0° printing angle. Therefore, it can be said that around 5–6 are the optimum value for the perimeter counts in this study.

To evaluate the obtained model, tensile tests were applied to the samples produced using different parameter values that are not included in Table 2, and the test results obtained, and the results predicted by the model equation are given in Table 4.

The percentage of error was determined with the help of the following equation:

$$\text{Error}(\%) = \left(\frac{\text{TS}_d - \text{TS}_t}{\text{TS}_d}\right) \times 100 \qquad \text{(Eq 5)}$$

where TS_d is the experimental tensile strength, TS_t is the predicted tensile strength by the model. TS_t values were calculated using the coded values (A: printing angle, B: infill density, C: perimeter count) with the help of the model equation (Eq. 4) stated above. From the results obtained, it is seen that the error percentages are low, and the related model can be used to estimate the tensile strength.

As a result, setting the printing angle as 90° and the infill density being full increases the tensile strength of the PLA produced. However, as seen in Table 2, these parameter values prolong the printing time and cause an increase in the amount of material used. Therefore, using the model equation obtained

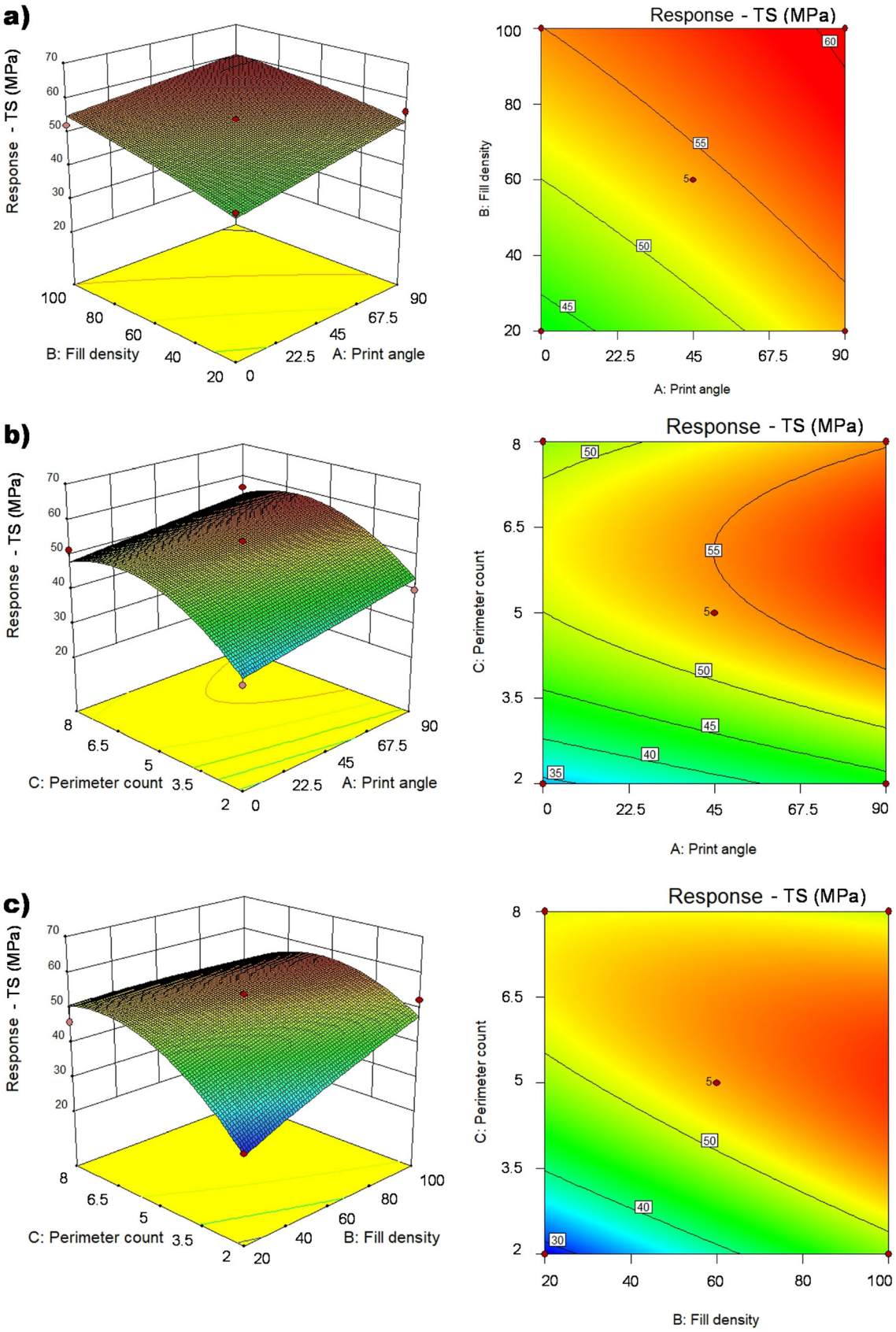

Fig. 9 Response surface plots and contour plots (a) print angle–infill density, (b) print angle–perimeter count, (c) infill density–perimeter count)

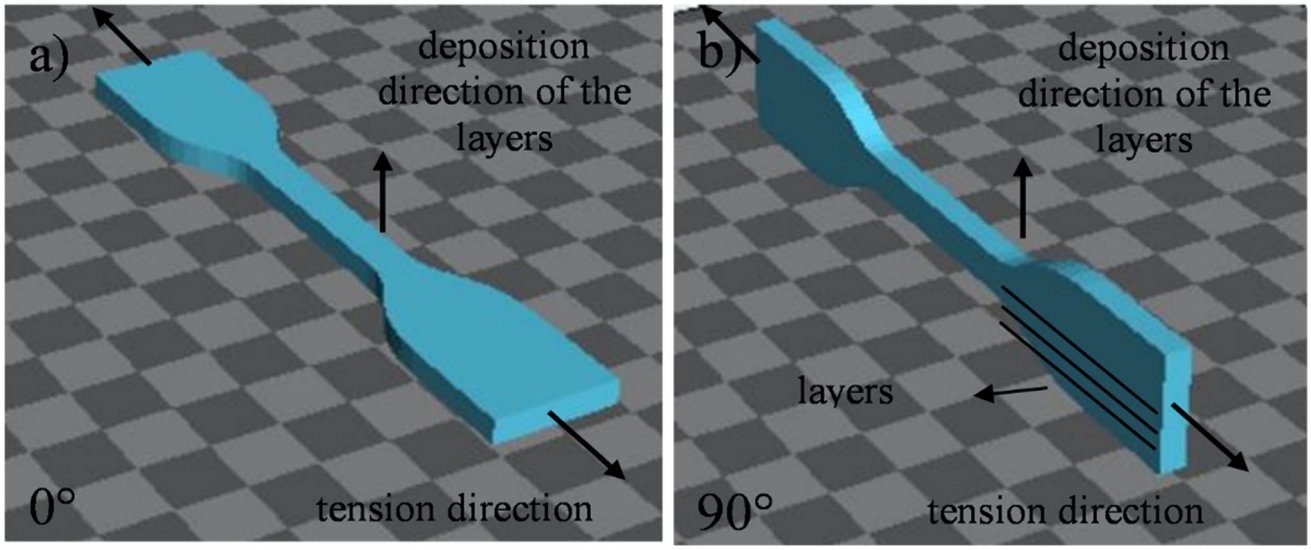

Fig. 10 Schematic view of the addition direction of the layers and tension direction (a) 0° print angle, (b) 90° print angle

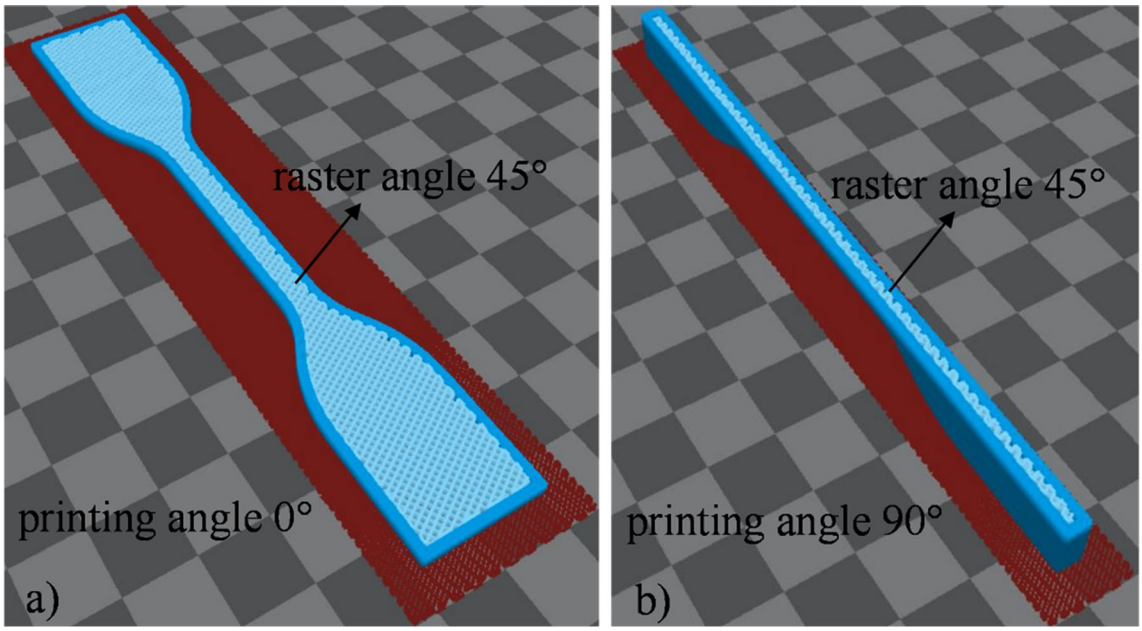

Fig. 11 Cross-sectional view of the printed specimen for the constant raster angle of 45° (a) 0° print angle and (b) 90° print angle

with the experimental design approach, it is possible to choose parameters suitable for the required tensile strength and effective in terms of time and material usage.

4. Conclusions

In this study, PLA tensile test specimens were produced by Zaxe X1 desktop 3D FDM printer, and the effects of printing angle, infill density, and perimeter count parameters on tensile strength were investigated. To evaluate the optimum printing parameters that will increase the strength, the experimental design method, RSM, was used. The proposed model equation was also evaluated by performing additional experiments outside the experimental design list. It showed that it could be used for strength estimation with low margins of error. According to the results obtained, it was seen that the 90° printing angle, 100% infill density, and the perimeter count around 5–6 maximized the tensile strength. However, the increase in filling density increased the amount of material used and printing times. With the help of the proposed model equation and the contour plots obtained, it is possible to print samples in shorter times and using less material by selecting the

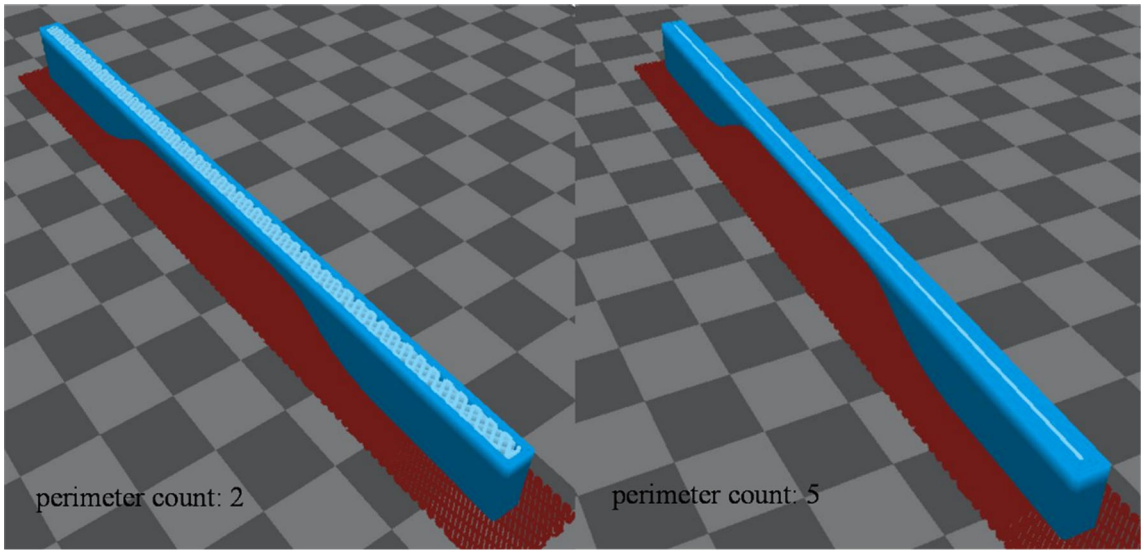

Fig. 12 Increase in perimeter count resulting in fibers in the cross section, which is parallel to the loading axis, instead of the filled region with 45° raster angle

Table 4 Error evaluation of the model with new experiments

Printing angle	Infill density	Perimeter count	A	B	C	Tensile strength, experimental, MPa	Tensile strength, predicted, MPa	Error, %
90	40	3	1	− 0.5	− 0.667	47.10	46.37	1.55
0	40	3	− 1	− 0.5	− 0.667	34.87	36.45	− 4.53
0	80	6	− 1	0.5	0.333	51.77	53.18	− 2.72

printing parameters that can provide the optimum tensile strength according to the requirement.

Acknowledgments

The author thanks Marmara University for its infrastructural support.

References

1. D. Dev Singh, T. Mahender, and A. Raji Reddy, Powder Bed Fusion Process: A Brief Review, *Mater. Today Proc.*, 2021, **46**, p 350–355. https://doi.org/10.1016/j.matpr.2020.08.415
2. K.V. Wong and A. Hernandez, A Review of Additive Manufacturing, *ISRN Mech. Eng.*, 2012, **2012**, p 208760. https://doi.org/10.5402/2012/208760
3. H.D. Vora and S. Sanyal, A Comprehensive Review: Metrology in Additive Manufacturing and 3D Printing Technology, *Prog. Addit. Manufact.*, 2020 https://doi.org/10.1007/s40964-020-00142-6
4. O. Santoliquido, P. Colombo, and A. Ortona, Additive Manufacturing of Ceramic Components by Digital Light PROCESSING: A Comparison Between the "Bottom-up" and the "Top-Down" Approaches, *J. Eur. Ceram. Soc.*, 2019, **39**, p 2140–2148. https://doi.org/10.1016/j.jeurceramsoc.2019.01.044
5. Y. Wu, Y. Lu, M. Zhao, S. Bosiakov, and L. Li, A Critical Review of Additive Manufacturing Techniques and Associated Biomaterials Used in Bone Tissue Engineering, *Polymers (Basel)*, 2022, **14**(10), p 2117. https://doi.org/10.3390/polym14102117
6. O.A. Mohamed, S.H. Masood, and J.L. Bhowmik, Optimization of Fused Deposition Modeling Process Parameters: A Review of Current Research and Future Prospects, *Adv. Manufact.*, 2015, **3**, p 42–53. https://doi.org/10.1007/s40436-014-0097-7
7. S. Vyavahare, S. Teraiya, D. Panghal, and S. Kumar, Fused Deposition Modelling: A Review, *Rapid Prototyp. J.*, 2020, **26**, p 176–201. https://doi.org/10.1108/RPJ-04-2019-0106
8. R.B. Kristiawan, F. Imaduddin, D. Ariawan, Ubaidillah, Z. Arifin, A review on the fused deposition modeling (FDM) 3D printing: Filament processing, materials, and printing parameters, Open Engineering, 2021, 11, p 639-649. https://doi.org/10.1515/eng-2021-0063
9. M.Z. Huang, J. Nomai, and A.K. Schlarb, The Effect of Different Processing, Injection Molding (IM) and Fused Deposition Modeling (FDM), on the Environmental Stress Cracking (ESC) Behavior of Filled and Unfilled Polycarbonate (PC), *Express Polym Lett.*, 2021, **15**, p 194–202. https://doi.org/10.3144/expresspolymlett.2021.18
10. F.A. Santos, H. Rebelo, M. Coutinho, L.S. Sutherland, C. Cismasiu, I. Farina, and F. Fraternali, Low Velocity Impact Response of 3D Printed Structures Formed by Cellular Metamaterials and Stiffening Plates: PLA vs. PETg, *Compos. Struct.*, 2021, **256**, p 113128. https://doi.org/10.1016/j.compstruct.2020.113128
11. N. Singh, R. Singh, I.P.S. Ahuja, I. Farina, and F. Fraternali, Metal Matrix Composite from Recycled Materials by Using Additive Manufacturing Assisted Investment Casting, *Compos. Struct.*, 2019, **207**, p 129–135. https://doi.org/10.1016/j.compstruct.2018.09.072
12. Y. Ramot, M. Haim-Zada, A.J. Domb, and A. Nyska, Biocompatibility and Safety of PLA and its Copolymers, *Adv. Drug Deliv. Rev.*, 2016, **107**, p 153–162. https://doi.org/10.1016/j.addr.2016.03.012
13. N. Naveed, Investigate the Effects of Process Parameters on Material Properties and Microstructural Changes of 3D-printed Specimens using Fused Deposition Modelling (FDM), *Mater. Technol.*, 2021, **36**, p 317–330. https://doi.org/10.1080/10667857.2020.1758475
14. H. Liu, X. Cheng, X.H. Yang, G.M. Zheng, and Q.J. Guo, Experimental Study on Parameters of 3D Printing Process for PEEK Materials, *IOP Conf. Ser. Mater. Sci. Eng.*, 2019, **504**, p 012001. https://doi.org/10.1088/1757-899X/504/1/012001

15. O.A. Mohamed, S.H. Masood, and J.L. Bhowmik, Mathematical Modeling and FDM Process Parameters Optimization Using Response Surface Methodology Based on Q-Optimal Design, *Appl. Math. Model.*, 2016, **40**, p 10052–10073. https://doi.org/10.1016/j.apm.2016.06.055
16. S. Khan, K. Joshi, and S. Deshmukh, A Comprehensive Review on Effect of Printing Parameters on Mechanical Properties of FDM Printed Parts, *Mater. Today: Proc.*, 2022, **50**, p 2119–2127. https://doi.org/10.1016/j.matpr.2021.09.433
17. O.A. Mohamed, S.H. Masood, J.L. Bhowmik, M. Nikzad, and J. Azadmanjiri, Effect of Process Parameters on Dynamic Mechanical Performance of FDM PC/ABS Printed Parts Through Design of Experiment, *J. Mater. Eng. Perform.*, 2016, **25**, p 2922–2935. https://doi.org/10.1007/s11665-016-2157-6
18. S. Wang, Y. Ma, Z. Deng, S. Zhang, and J. Cai, Effects of Fused Deposition Modeling Process Parameters on Tensile, Dynamic Mechanical Properties of 3D Printed Polylactic Acid Materials, *Polym. Test.*, 2020, **86**, p 106483. https://doi.org/10.1016/j.polymertesting.2020.106483
19. P. Demircioglu, H.S. Sucuoglu, I. Bogrekci, and A. Gultekin, The Effect of Three Dimensional Printed Infill Pattern on Structural Strength, *EL-Cezeri J. Sci. Eng.*, 2018, **5**, p 785–796. https://doi.org/10.31202/ecjse.423915
20. A.W. Gebisa and H.G. Lemu, Influence of 3D Printing FDM Process Parameters on Tensile Property of ULTEM 9085, *Proc. Manufact.*, 2019, **30**, p 331–338. https://doi.org/10.1016/j.promfg.2019.02.047
21. M.S. Kamer, Ş Temiz, D.H. Yaykaşli, A. Kaya, and O. Akay, 3B Yazıcıda Farklı Yazdırma Hızlarında ABS ve PLA Malzeme Ile Üretilen Çekme Test Numunelerinin Mekanik Özelliklerinin Karşılaştırılması (Comparison of Mechanical Properties of Tensile Test Specimens Produced with ABS and PLA Material at Different Printing Speeds in 3D Printer), *Gazi Üniversitesi Mühendislik-Mimarlık Fakültesi Dergisi*, 2022, **37**, p 1197–1211. https://doi.org/10.17341/gazimmfd.961981. (**in Turkish**)
22. O. Doğan and M.S. Kamer, Farklı Üretim Parametreleri Kullanılarak 3B Yazıcı Ile Üretilen Test Numunelerinin Sürünme Davranışlarının Deneysel Olarak Incelenmesi (Experimental Investigation of the Creep Behavior of Test Specimens Manufactured with Fused Filament Fabrication Using Different Manufacturing Parameters), *Gazi Üniversitesi Mühendislik-Mimarlık Fakültesi Dergisi*, 2023, **38**, p 1839–1848. https://doi.org/10.17341/gazimmfd.1122973. (**in Turkish**)
23. T. Lundstedt, E. Seifert, L. Abramo, B. Thelin, Å. Nyström, J. Pettersen, and R. Bergman, Experimental Design and Optimization, *Chemom. Intell. Lab. Syst.*, 1998, **42**, p 3–40. https://doi.org/10.1016/S0169-7439(98)00065-3
24. V. Yiga, M. Lubwama, P. Olupot, Application of Response Surface Methodology for Optimizing Tensile Strength of Rice Husk Fiber-Reinforced Polylactic Acid Composites, Mater. Proc., 2021, 3
25. S.L.C. Ferreira, R.E. Bruns, H.S. Ferreira, G.D. Matos, J.M. David, G.C. Brandão, E.G.P. da Silva, L.A. Portugal, P.S. dos Reis, A.S. Souza, and W.N.L. dos Santos, Box-Behnken Design: An Alternative for the Optimization of Analytical Methods, *Anal. Chim. Acta*, 2007, **597**, p 179–186. https://doi.org/10.1016/j.aca.2007.07.011
26. U. Balaji and S.K. Pradhan, Titanium Anodisation Designed for Surface Colouration - Systemisation of Parametric Interaction Using Response Surface Methodology, *Mater. Des.*, 2018, **139**, p 409–418. https://doi.org/10.1016/j.matdes.2017.11.026
27. A.T.M.A.M. Joglekar, Product Excellence through the Design of Experiments, *Cereal Food World*, 1987, **32**, p 857–868.
28. G.D. Okçu, N.B. Pakdil, H.E. Ökten, and A. Yalçuk, A Box-Behnken Design (BBD) Optimization of the Photocatalytic Degradation of 2,4-Dichlorophenoxyacetic Acid (2,4-D) Using TiO2/H2O2, *Desalin. Water Treat.*, 2018, **123**, p 186–195. https://doi.org/10.5004/dwt.2018.22681
29. V.A. Yiga, M. Lubwama, S. Pagel, P.W. Olupot, J. Benz, and C. Bonten, Optimization of Tensile Strength of PLA/clay/rice Husk Composites Using Box-Behnken Design, *Biomass Convers. Biorefinery*, 2021 https://doi.org/10.1007/s13399-021-01971-3
30. M.-H. Hsueh, C.-J. Lai, C.-F. Chung, S.-H. Wang, W.-C. Huang, C.-Y. Pan, Y.-S. Zeng, and C.-H. Hsieh, Effect of Printing Parameters on the Tensile Properties of 3D-Printed Polylactic Acid (PLA) Based on Fused Deposition Modeling, *Polymers*, 2021, **13**, p 2387.
31. S.H. Ahn, C. Baek, S. Lee, and I.S. Ahn, Anisotropic Tensile Failure Model of Rapid Prototyping Parts - Fused Deposition Modeling (FDM), *Int. J. Mod Phys B*, 2003, **17**, p 1510–1516. https://doi.org/10.1142/S0217979203019241
32. S. Srinivasan Ganesh Iyer, and O. Keles, Effect of Raster Angle on Mechanical Properties of 3D Printed Short Carbon Fiber Reinforced Acrylonitrile Butadiene Styrene, *Compos. Commun.*, 2022, **32**, p 101163. https://doi.org/10.1016/j.coco.2022.101163
33. G.M. Liseli Baich and H. Marie, Study of Infill Print Design on Production Cost-Time of 3D Printed ABS Parts, *Int. J. Rapid Manufact.*, 2015, **5**, p 308–319. https://doi.org/10.1504/ijrapidm.2015.074809
34. W.C. Miguel Fernandez Vicente, S. Ferrandiz, and A. Conejero, Effect of Infill Parameters on Tensile Mechanical Behavior in Desktop 3D Printing, *3D Print. Addit. Manufact.*, 2016, **3**, p 183–192. https://doi.org/10.1089/3dp.2015.0036
35. J. Klingenbeck, A. Lion, and M. Johlitz, On the Influence of Perimeter, Infill-Direction and Geometry on the Tensile Properties of Test Specimen Manufactured by Fused Filament Fabrication, *Lectures Notes on Advanced Structured Materials*. H. Altenbach, M. Johlitz, M. Merkel, A. Öchsner Ed., Springer International Publishing, Cham, 2022, p 167–182
36. C. Lubombo and M.A. Huneault, Effect of Infill Patterns on the Mechanical Performance of Lightweight 3D-Printed Cellular PLA Parts, *Mater. Today Commun.*, 2018, **17**, p 214–228. https://doi.org/10.1016/j.mtcomm.2018.09.017